University of Bath

Alternative formats

If you require this document in an alternative format, please contact:
openaccess@bath.ac.uk

Title:

Impact localisation on a composite tail rotor blade using an inverse filtering approach.

Authors:

Francesco Ciampa and Michele Meo[1]

Material Research Centre, Department of Mechanical Engineering, University of Bath,

Bath, BA2 7AY, UK

Running title:

Imaging of the impact location on a composite tail rotor blade.

[1] Correspondent author: m.meo@bath.ac.uk

Abstract

This paper presents an *in-situ* Structural Health Monitoring (SHM) imaging system for the localization of impacts on a composite complex structure such as a tail rotor blade. Unlike conventional plate-like panels, this composite structure presents a strong anisotropy and inhomogeneous elastic nature due to the presence of both glass fibre and carbon fibre, a geometrically complex shape due to the curvature of the blade's airfoil section, and variations of the mechanical behaviour due to local changes of the thickness. The proposed imaging technique is based on the inverse filtering or reciprocal time reversal approach applied to the waveforms originated from a point of the structure of unknown location (impact source), and a number of signals stored into a database containing the experimental Green's function of the medium. Unlike other ultrasonic impact localization methods, the present technique allows achieving the optimal focalization of the impact point in the spatial and time domain, by taking advantage of multiple linear scattering and a small number of receiver sensors.

I. INTRODUCTION

Developments in carbon fibres reinforced plastic (CFRP) and glass fibres (GFRP) materials have allowed a radical advancement in lightweight aerospace applications such as rotor blade design. Indeed, laminated composite structures can be tailored to display desired properties in specific directions and areas, such as high stiffness and strength. However, these components are sensitive to low velocity impact damages that can considerably degrade the structural integrity and, if not detected, they can result in loss of control and catastrophic failures of the vehicle. Hence, impact localization has become an important tool for Structural Health Monitoring (SHM) systems based on ultrasonic guided waves (GW). A number of algorithm-based methods have been developed in the past for the localization of the acoustic emission (AE) source in isotropic and anisotropic plate-like structures [1], [2], [3], [4]. Most of these techniques rely on time of arrival (TOA) identification and the group velocity determination of the coherent part of the wave field (ballistic wave) reaching a network of transducers bonded on the structures. Usually, advanced signal processing technique such as peak detection [5], cross-correlation [6], Hilbert [7] and wavelet transformation [8] can be employed to extract physical parameters from measured data, and then to use them to detect the impact location. However, the dispersive nature of GW and the presence of multiple scattering, mode conversion and reflection from the boundaries (*diffuse wave field*) can lead to waveforms recorded from the sensors dissimilar from the original elastic source. In other words, the effects of wave propagation in geometrically complex structures can degrade the quality of the TOA estimation, causing poor localization. To overcome these limitations, Time Reversal (TR) process has been used as a tool for the imaging of the impact source in solid media [9], [10]. Indeed, in a TR experiment, due to the time

3

invariance and spatial reciprocity of linear wave equation, an input signal can be focused back on the original source if the output received by a set of transducers is time reversed and emitted onto the excitation point. The first improvement of TR process is to compensate the dispersive behaviour of GW [10]. Indeed, depending on the propagation frequency, dispersive GW have a number of wave packets that travel at higher and lower speeds toward the receiver sensor. After a TR process, the slower modes are emitted first, so that all the waveforms can converge at the original source point at the same time, thus compensating dispersion. However, the refocusing of TR holds only in the case of lossless media. Indeed, from the study of the elastodynamic wave equation, TR invariance is due to the presence of the even order (second order) time partial derivative operator. This condition cannot be fulfilled in dissipative media, as the wave equation presents a time partial derivative operator of the first order [12]. That is, material dissipations can generate amplitude distortions of the propagating wave front and TR behaviour become difficult to be predicted. Nevertheless, TR can be easily converted to reciprocal TR or Inverse Filtering (IF) by inverting the impulsive response of the structure (Fourier transform of the Green's function). This simple but effective operation, allows recovering the optimal focusing, even in dissipative media [13].

The objective of the work is to report, both theoretically and experimentally, an *in-situ* Structural Health Monitoring (SHM) system able to identify the occurrence and location of low velocity impacts in a "real" aerospace component. In particular, this research study extended a recent work published by the same authors on the localization of the impact source in a reverberant plate-like structure, to a complex construction such as a tail rotor blade of the Agusta-Westland helicopter. Indeed, unlike conventional plate-like panels, this composite structure presents a strong anisotropy and inhomogeneous elastic nature

4

due to the presence of a double material (CFRP and GFRP), a geometrically complex shape due to the curvature of the blade airfoil section and rivets, and variations of the mechanical behaviour due to local changes of the thickness. The proposed imaging technique is based on the IF approach applied to the waveform originated from a point of the structure of unknown location (impact source), and a number of signals stored into a database containing the experimental Green's function of the medium. Unlike other ultrasonic impact localization methods, the present method allows achieving the optimal focalization of the impact point in the spatial and time domain, by taking advantage of multiple linear scattering and a small number of receiver sensors.

The layout of this paper is as follows: in Section II, the imaging method for the localization of the impact source is theoretically presented. In Section III, the benefits of a reverberant fully diffuse wave field on the imaging process using IF are illustrated. Section IV reports the experimental set-up whilst Section V illustrates the imaging results for a number of impact points. Then, the conclusions of the paper are presented.

II. THEORETICAL ANALYSIS OF RECIPROCAL TIME REVERSAL

If the time reversal invariance and spatial reciprocity of the elastodynamic wave equation are satisfied, either TR or IF imaging process can be used to focus ultrasonic waves in diffuse wave fields and anisotropic media. The last technique, however, allows compensating some detrimental effects such as the limited transducer bandwidth and the material absorptions, in order to recover the optimal focusing at the impact source. In addition, according to Huygens's principle in diffraction theory [14], the reconstruction of the wave function in a generic volume at any time can be obtained by the knowledge of its sources located on a 2D surface. The reciprocal time reversal experiment is usually

split in two steps. In the first step a number of signals representing a library of impulse responses from *M* points ("excitation points") along the plane of the structure is recorded by one receiver transducer and stored (Fig. 1).
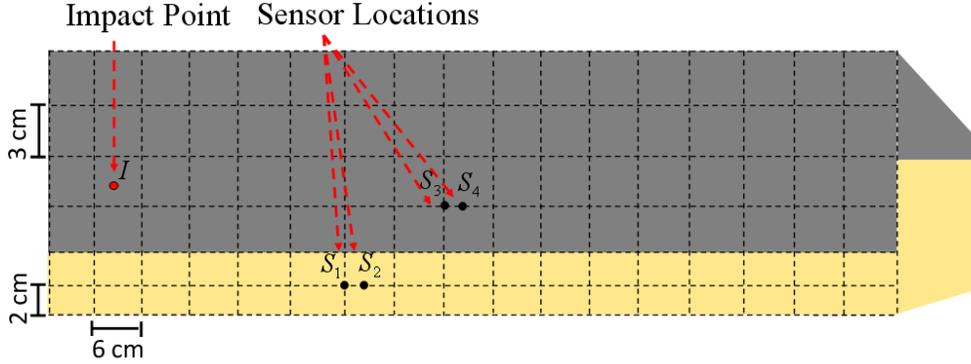

Figure 1 Architecture of the imaging method

The second step consists of the recognition of the optimal refocusing procedure at the source location. The basic idea is to correlate the impulsive transfer function associated to each excitation point with that of the new impact of unknown location. In this manner, the information on the AE source location is accomplished by the imaging process as the maximum of the correlation at the focus point (referred as "virtual IF experiment").

A. Elastodynamic Wave Equation with Dirac Point-like Source

Reciprocal TR theoretical description for elastic wave propagation involves exploiting properties of temporal and frequency convolution, Borel's theorem and Green's function theory. As a starting point, assuming the wave field $\psi(\mathbf{r},t)$, with $\mathbf{r} = x_1\hat{i} + x_2\hat{j} + x_3\hat{k}$ in Lagrangian coordinates x_j, as a generic component of the displacement vector field in the case of a solid, either elastically isotropic or anisotropic medium, we can write [15]:

$$c^2\nabla^2\psi(\mathbf{r},t) - \frac{\partial^2\psi(\mathbf{r},t)}{\partial t^2} = -e(\mathbf{r},t). \qquad (1)$$

6

Eq. (1) is an inhomogeneous, linear, partial differential equation (PDE) where c is a generic component of the velocity of propagation in the medium and $e(\mathbf{r},t)$ is the excitation of a known impulsive point-like source given by:

$$e(\mathbf{r},t) = \delta(\mathbf{r},t) \qquad (2)$$

where $\delta(\mathbf{r},t)$ represents the Dirac distribution in space and time domains. Eq. (2) is a causal function and the temporal excitation only exists on a finite time-interval $[0, T]$, where T is the temporal duration of the excitation function $e(\mathbf{r}, t)$. The time-derivative operator of Eq. (1) appears only at the second order, hence if $\psi(\mathbf{r}, t)$ is a solution, then $\psi(\mathbf{r},-t)$ is also a solution. It should also be noticed that the presence of the Lapalcian differential operator, guarantees the invariance of Eq. (1) under the transformation $\mathbf{r} \rightarrow -\mathbf{r}$, i.e. it guarantees a *spatial reciprocity condition*. According to the Green's theorem [16], to solve Eq. (1) it is useful to define a Green space-time function G that depends on the variables $(\mathbf{r},t;\mathbf{r}_0,t_0)$. Green's function allows the calculation of the wave field ψ at a given position and time $(\mathbf{r}, t)$ without explicitly solving the differential Eq. (1). From a mathematical point of view, Green's function has to satisfy the following conditions [17]:

- $G(\mathbf{r},t;\mathbf{r}_0,t_0)$ must be a solution to the following linear inhomogeneous differential equation:

$$c^2 \nabla^2 G(\mathbf{r},t;\mathbf{r}_0,t_0) - \frac{\partial^2 G(\mathbf{r},t;\mathbf{r}_0,t_0)}{\partial t^2} = -\delta(\mathbf{r}-\mathbf{r}_0)\delta(t-t_0) \qquad (3)$$

where $\delta(\mathbf{r}-\mathbf{r}_0)$ and $\delta(t-t_0)$ are Dirac delta functions in space and time, respectively. $G(\mathbf{r},t;\mathbf{r}_0,t_0)$ is the field produced in $\mathbf{r}$ at time t by an impulsive force located in $\mathbf{r}_0$ and excited at time t_0. For $t < t_0$ causality requires that $G(\mathbf{r},t;\mathbf{r}_0,t_0) \equiv 0$.

- $G(\mathbf{r},t;\mathbf{r}_0,t_0)$ is a reciprocal function in the sense of the *reciprocity theorem*:

$$G(\mathbf{r},t;\mathbf{r}_0,t_0) \equiv G(\mathbf{r}_0,t_0;\mathbf{r},-t) \equiv G(\mathbf{r}_0,t;\mathbf{r},t_0). \qquad (4)$$

- $G(\mathbf{r},t;\mathbf{r}_0,t_0)$ must satisfy the homogeneous boundary conditions on S (Dirichelet, Neumann or mixed):

$$G(\mathbf{r},t;\mathbf{r}_0,t_0) = 0 \quad \mathbf{r} \in S \qquad (5.1)$$

$$\frac{\partial G(\mathbf{r},t;\mathbf{r}_0,t_0)}{\partial \mathbf{n}} = 0 \quad \mathbf{r} \in S \qquad (5.2)$$

where S is a closed surface of a solid Ω, $\dfrac{\partial G(\mathbf{r},t;\mathbf{r}_0,t_0)}{\partial \mathbf{n}}$ is the Green's function normal derivative and $\mathbf{n}$ is the vector field normal to the closed surface in each of its points, directed outwards.

- $G(\mathbf{r},t;\mathbf{r}_0,t_0)$ must satisfy the Cauchy initial conditions:

$$G(\mathbf{r},t;\mathbf{r}_0,t_0) = 0 \quad t = t_0 \qquad (6.1)$$

$$\frac{\partial G(\mathbf{r},t;\mathbf{r}_0,t_0)}{\partial t} = 0 \quad t = t_0. \qquad (6.2)$$

Hence, considering Eq. (3) and conditions (5.1-6.2), the solution to the elastodynamic wave equation (1) can be expressed in terms of the Green's function, boundary conditions and initial condition as follows:

$$c^2 \nabla_0{}^2 \psi(\mathbf{r}_0,t_0) - \frac{\partial^2 \psi(\mathbf{r}_0,t_0)}{\partial t_0{}^2} = -e(\mathbf{r}_0,t_0) \qquad (7.1)$$

$$c^2 \nabla^2 G(\mathbf{r},t;\mathbf{r}_0,t_0) - \frac{\partial^2 G(\mathbf{r},t;\mathbf{r}_0,t_0)}{\partial t_0{}^2} = -\delta(\mathbf{r}-\mathbf{r}_0)\delta(t-t_0). \qquad (7.2)$$

Multiplying Eq. (7.1) by $G(\mathbf{r},t;\mathbf{r}_0,t_0)$ and Eq. (7.2) by $\psi(\mathbf{r}_0,t_0)$, performing the difference

and then integrating over the solid Ω_0 and over the time t_0 from 0 to t', with $t' \gg t$ in

order to avoid the integration exactly at the peak of the delta function, we obtain:

$$
\begin{aligned}
&\int_0^{t'} dt_0 \iiint_\Omega \Big\{ c^2 \Big[\nabla_0{}^2 \psi(\mathbf{r}_0,t_0) G(\mathbf{r},t;\mathbf{r}_0,t_0) - \nabla_0{}^2 G(\mathbf{r},t;\mathbf{r}_0,t_0)\psi(\mathbf{r}_0,t_0) \\
&\quad + \frac{\partial^2 G(\mathbf{r},t;\mathbf{r}_0,t_0)}{\partial t_0{}^2}\psi(r_0,t_0) - \frac{\partial^2 \psi(\mathbf{r}_0,t_0)}{\partial t_0{}^2}G(\mathbf{r},t;\mathbf{r}_0,t_0) \Big] \Big\} d\Omega_0 \\
&= \int_0^{t'} dt_0 \iiint_\Omega \big[\delta(\mathbf{r}-\mathbf{r}_0)\delta(t-t_0)\psi(\mathbf{r}_0,t_0) - f(\mathbf{r}_0,t_0)G(\mathbf{r},t;\mathbf{r}_0,t_0) \big] d\Omega_0 \\
&= \psi(\mathbf{r},t) - \int_0^{t'} dt_0 \iiint_\Omega \big[e(\mathbf{r}_0,t_0)G(\mathbf{r},t;\mathbf{r}_0,t_0) \big] dV_0
\end{aligned}
\qquad (8)
$$

The volume integral over the two terms in left side of Eq. (8) involving Laplaceans, turns

into a surface integral employing Green's second identity as follows:

$$
\begin{aligned}
&\iiint_\Omega \Big[\frac{\partial G(\mathbf{r},t;\mathbf{r}_0,t_0)}{\partial t_0}\psi(\mathbf{r}_0,t_0) - \frac{\partial \psi(\mathbf{r}_0,t_0)}{\partial t_0}G(\mathbf{r},t;\mathbf{r}_0,t_0) \Big] d\Omega_0 \\
&+ \int_0^{t'} dt_0 \iint_S c^2 \big[\nabla_0 \psi(\mathbf{r}_0,t_0)G(\mathbf{r},t;\mathbf{r}_0,t_0) - \nabla_0 G(\mathbf{r},t;\mathbf{r}_0,t_0)\psi(\mathbf{r}_0,t_0) \big] \cdot \mathbf{n}\, dS_0
\end{aligned}
\qquad (9)
$$

Hence, Eq. (9) can be rewritten as:

$$\psi(\mathbf{r},t) = g(\mathbf{r},t) + h(\mathbf{r},t) + s(\mathbf{r},t) \qquad (10)$$

where:

$$g(\mathbf{r},t) = \int_0^{t'} dt_0 \iiint_\Omega \left[e(\mathbf{r}_0,t_0) G(\mathbf{r},t;\mathbf{r}_0,t_0) \right] d\Omega_0$$

$$h(\mathbf{r},t) = c^2 \int_0^{t'} dt_0 \iint_S \left\{ \left[G(\mathbf{r},t;\mathbf{r}_0,t_0) \nabla_0 \psi(\mathbf{r}_0,t_0) - \nabla_0 G(\mathbf{r},t;\mathbf{r}_0,t_0) \psi(\mathbf{r}_0,t_0) \right] \cdot \mathbf{n}(\mathbf{r}_0) \right\} dS_0 .$$

$$s(\mathbf{r},t) = \iiint_\Omega \left[\frac{\partial G(\mathbf{r},t;\mathbf{r}_0,t_0)}{\partial t_0} \psi(\mathbf{r}_0,t_0) - \frac{\partial \psi(\mathbf{r}_0,t_0)}{\partial t_0} G(\mathbf{r},t;\mathbf{r}_0,t_0) \right] d\Omega_0$$

Eq. (10) gives the complete solution of the inhomogeneous problem (1) including the initial conditions. The above terms $g(\mathbf{r},t)$ and $h(\mathbf{r},t)$ represent the effect of the source and the boundary conditions, respectively. The last term $s(\mathbf{r},t)$ is related only to the initial conditions [16]. Assuming a free unbounded space, supposing that we are able to measure at any point of a closed surface S the wave field $\psi(\mathbf{r},t)$ and its normal derivatives (set to zero at infinity), the general solution of the elastodynamic wave equation (1) takes the form:

$$\psi(\mathbf{r},t) = \int_0^{t'} dt_0 \iiint_\Omega \left[e(\mathbf{r}_0,t_0) G(\mathbf{r},t;\mathbf{r}_0,t_0) \right] d\Omega_0 =$$
$$= \iiint_\Omega \left[G(\mathbf{r},t;\mathbf{r}_0) \underset{t}{\otimes} e(\mathbf{r}_0,t) \right] d\Omega_0 \tag{11}$$

where the symbol $\underset{t}{\otimes}$ represents a convolution over time (note that $t=t_0=0$ for causality reasons). Eq. (11) represents a linear combination of the acoustic field and its normal derivatives measured by the receiver sensor located in $\mathbf{r}$ at time t by an impulsive force located in $\mathbf{r}_0$. Substituting Eq. (2) in (11), the above equation represents a particular case of the Borel's theorem, in which the excitation function is the Dirac delta function. Therefore, only in this particular case, the wave field acquired by the sensor is equal to the structural impulsive response.

In the first step, impact loads are applied in points arbitrarily chosen on the plane of the structure ("focusing plane"), in order to create a database of impulse responses from different locations $\mathbf{r}_m$. In other words, the surface of the structure is converted in a discrete domain composed by M "excitation points", and the spatial integral of Eq. (11) is turned into a sum over the "focusing plane" as follows:

$$\psi(\mathbf{r},t) = \sum_{m=1}^{M} G(\mathbf{r},t;\mathbf{r}_m) \underset{t}{\otimes} e(\mathbf{r}_m,t).$$

(12)

In the frequency domain, Eq. (12) is (the sum tem is omitted for clarity reasons):

$$\hat{\psi}(\mathbf{r},\omega) = \hat{G}(\mathbf{r},\omega;\mathbf{r}_m)\hat{e}(\mathbf{r}_m,\omega)$$

(13)

where the symbol $\hat{}$ corresponds to a Fourier transformation operation and

$\hat{G}(\mathbf{r},\omega;\mathbf{r}_m) = \int\limits_{-\infty}^{+\infty} G(\mathbf{r},t;\mathbf{r}_m) e^{-j\omega t} dt$ is the impulsive transfer function of the system from each

of the m $(1 \le m \le M)$ excitation points. In particular, $\hat{G}(\mathbf{r},\omega;\mathbf{r}_m)$ represents the amplitude of the ith mode contained in the structural response due to impulsive excitation. On the other hand, according to the *spatial reciprocity condition* [Eq. (4)], $\hat{G}(\mathbf{r}_m,\omega;\mathbf{r})$ corresponds to the inverse propagation from the receiver transducer to the mth excitation point. It should be noted that in matrix notation, this condition corresponds to a transposition operation. Hence, the M impulse responses are recorded and stored in a memory.

B. Reciprocal Time Reversal Focusing Approach

Classical TR experiment can be obtained by time reversing the received signals during the first step, i.e. throughout the transformation $t \Rightarrow T - t$. From a mathematical point of

view, this means that we are able to create secondary source on the surface of the structure, such that the boundary conditions on S are the time reversal component of the wave field $\psi(\mathbf{r},t)$ received during the first step [18]. In a more practical case, the second step of a reciprocal TR process is "virtually" performed in the computer. In particular, it consists of correlating the waveform emitted by a point of unknown location $\mathbf{r}_{m0}$ with all the impulse responses stored in the memory. Hence, a new impact is applied in one of the points of the focusing plane and its impulse response is measured by the same receiver sensor used in the first step. Therefore, the new spectral distribution $\hat{\psi}_{new}(\mathbf{r},\omega)$ measured by the receiver, when the impact $\hat{e}(\mathbf{r}_{m0},\omega)$ is generated, can be obtained as follows [13]:

$$\hat{\psi}(\mathbf{r},\omega) = \tilde{G}(\mathbf{r},\omega;\mathbf{r}_{m0})\hat{e}(\mathbf{r}_{m0},\omega) \qquad (14)$$

where $\tilde{G}(\mathbf{r},\omega;\mathbf{r}_{m0}) = \left[\hat{G}(\mathbf{r},\omega;\mathbf{r}_{m0})\right]^{*}\Big/\left\|\hat{G}(\mathbf{r},\omega;\mathbf{r}_{m0})\right\|^{2}$ is the inversion of the impulsive transfer function $\hat{G}(\mathbf{r},\omega;\mathbf{r}_{m0})$. The asterisk denotes complex conjugate operation (that is equivalent to a time reversal operation in the time domain) and $\left\|\hat{G}(\mathbf{r},\omega;\mathbf{r}_{m0})\right\|^{2}$ is the squared norm of the impulsive response, representing the square modal energy of the system. The effect of weighting the impulsive transfer function acquired in the second step is to create a "whitening process", wherein the number of modes employed for the back propagation can be increased. Indeed, the modes with weak and strong amplitude are emitted back at higher and lower energies, respectively. In this manner, the material dissipation can be compensated and the contrast can be enhanced [19]. That is, the optimal focusing at the impact source is performed through a "virtual" IF experiment, which relies on calculating the maxima correlation coefficients given by the following equation:

$$\hat{e}_{IF}(\mathbf{r}_m, \omega) = \hat{G}(\mathbf{r}_m, \omega; \mathbf{r})\widetilde{G}(\mathbf{r}, \omega; \mathbf{r}_{m0})\hat{e}(\mathbf{r}_{m0}, \omega) \qquad (15)$$

where the operator $\hat{G}(\mathbf{r}_m, \omega; \mathbf{r})\widetilde{G}(\mathbf{r}, \omega; \mathbf{r}_{m0})$ is called the *IF operator*. The maxima correlation coefficients are used to create a 2D map representing the structural surface, and the maximum of $\hat{e}_{IF}(\mathbf{r}_{m0}, \omega)$, i.e. when $\mathbf{r}_m = \mathbf{r}_{m0}$, allows obtaining the image of the impact source at the focus point.

III. INFLUENCE OF DIFFUSE WAVEFIELD ON THE IMAGING PROCESS

From a statistical point of view, fully diffuse wave field are characterized by a superposition of different fields with uncorrelated amplitude and random direction of propagation and phase [20]. Furthermore, in complex structures such as the tail rotor blade tested, the measured signals are typically non-stationary and feature an exponentially decaying "coda" which is dominated by multiple scattering (Fig. 2).
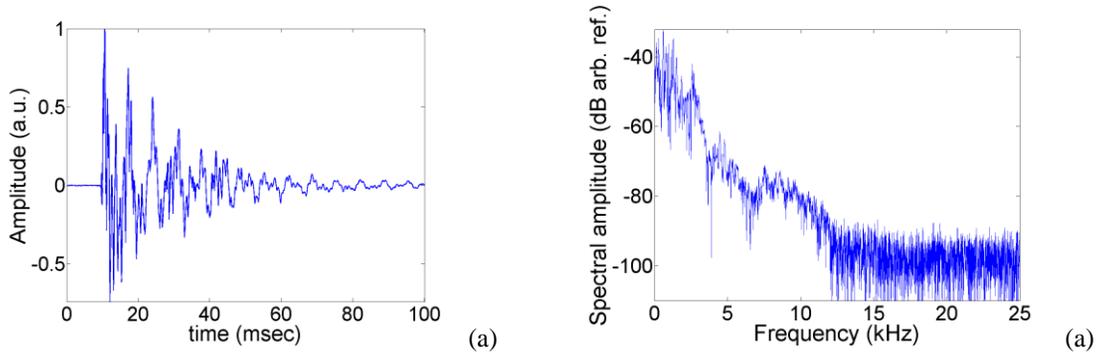

Figure 2 Normalized time history in one of the excitation points (a) and its frequency content (b)

In particular, the presence of heterogeneities such as a composite double material (CFRP and GFRP), local variations of the thickness and the curvature of the rotor blade airfoil influence the acoustic properties of the structure, generating reverberations within the medium. In this section, we propose to analyze the IF experiment in terms of Correlation

of a Diffuse Field (CDF). This concept has been widely used in seismology to retrieve the structural impulse response at two sensors locations [21] and only recently, it has been examined through a time reversal process [22]. In particular, in a reciprocal TR experiment, CDF is defined as the inverse Fourier transformation of the IF operator at $\mathbf{r}_m = \mathbf{r}_{m0}$:

$$
\begin{aligned}
CDF &= \frac{1}{\left\| G(\mathbf{r},t\,;\mathbf{r}_{m0}) \right\|^2} G(\mathbf{r}_{m0},t\,;\mathbf{r}) \underset{t}{\otimes} G(\mathbf{r},-t\,;\mathbf{r}_{m0}) \\
&= \frac{1}{\left\| G(\mathbf{r},t\,;\mathbf{r}_{m0}) \right\|^2} \int_{-\infty}^{+\infty} G(\mathbf{r}_{m0},t\,;\mathbf{r}) G(\mathbf{r},t+\tau\,;\mathbf{r}_{m0}) d\tau
\end{aligned}
\tag{16}
$$

where the right term of the above equation represents the cross-correlation of the Green's function of the system. The above equation is maximum at the focusing time $t=0$ and equal to the energy of the impulsive function $G(\mathbf{r},t\,;\mathbf{r}_{m0})$. Although a fully diffuse wave field is negative for impact localization techniques based on the TOA estimation, in the IF process the presence of reverberations becomes extremely important to image the impact source. In other words, in real applications where the waveforms under analysis are very dispersive, the cross-correlation function may cease to work for techniques that rely on the TOA measurement of the ballistic wave. Conversely, in the IF process [Eq. 16], as the entire signal is needed for the back propagation, a fully diffuse wave field improves the focusing at the original source. From a physical point of view, this concept can be explained in terms of conversion of the modes with complex wave number into modes with real wave number. Indeed, multiple scattering in a complex medium behave like "mirrors", allowing the non-propagating (evanescent) modes to be converted into propagating modes. In this manner, they can reach the far field where the receiver sensor is located, thus carrying additional information on the impact location. The result of such

operation, known as *kaleidoscopic effect*, creates a virtual enlargement of the transducer angular aperture, enabling a radical reduction of the number of transducers [23]. Therefore, the number of sensors employed is not related to the construction of a baseline to take into account the anisotropic features of the composite structures in each direction, as misinterpreted by Qui et al. [24], but simply to create a database of waveforms needed for the virtual IF process. Indeed, the same methodology would be valid for a reverberant isotropic structure. That is, only one receiver transducer can be used to acquire the signals.

IV. EXPERIMENTAL SET-UP

The experiments were carried out on a composite tail rotor blade (125 cm x 20 cm x 2 cm) provided by Agusta-Westland (Fig. 3).
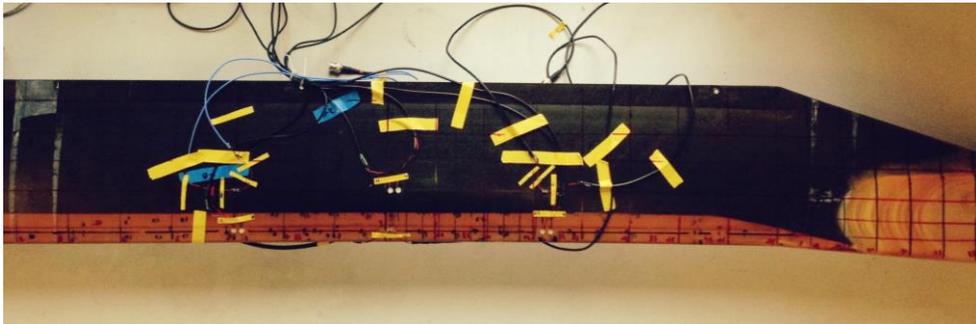

Figure 3 Image of the composite tail rotor blade tested

Although no quantitative information was given by the manufacturer regarding the blade, a number of assumptions were made on the structural make-up (Fig. 4a).
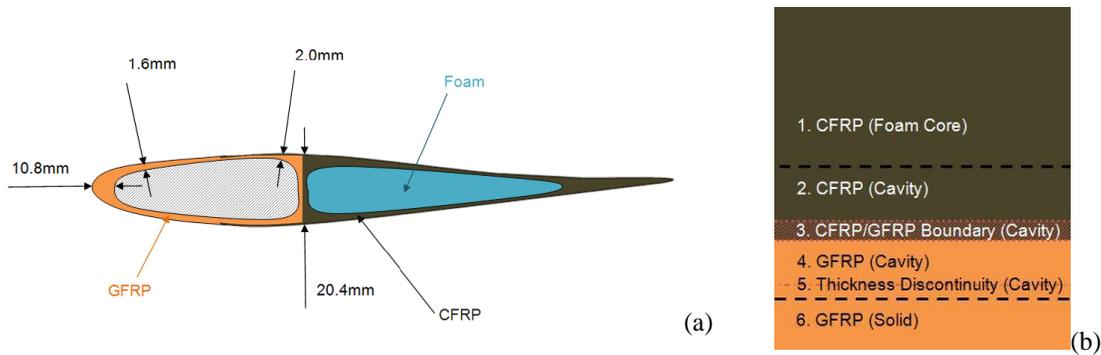
Figure 4 Composite rotor blade schematic (a) and region of interest on the surface (b)

In particular, the leading edge of the blade is made of GFRP for impact damage tolerance, whilst CFRP has been used for the rest of the blade to increase the structural strength and stiffness. The section of the blade is split into two parts by a CFRP spar web. The leading edge section is a cavity and the trailing edge section is filled with foam. In addition, the surface of the blade was divided into six distinct regions, as shown in Fig. 4b, based on the expected behaviour of the propagating GW. The dashed black lines mark the boundaries of the leading edge cavity space into which sensors could be placed in practical applications. The greatest complications were expected in region 3, the CFRP/GFRP boundary region, where the number of CFRP plies was reduced incrementally until GFRP made up the surface. It was not known what effect this would have on GW propagating through it. The passive sensors employed were four piezoelectric transducers (APC sensors) with diameter of 6.35 mm, thickness of 2.5 mm and central frequency of 100 kHz (broadband spectrum), mainly used for ultrasonic applications. The waveforms were acquired using an oscilloscope (Picoscope 4224) with a sampling rate of 99.5 kHz. From the time histories and the associated spectra (Fig. 2), the main energy of the amplitude spectrum of the waves induced by an uncontrolled system (modal hammer) was confined below 12 kHz. All the impacts were carried out manually in order to avoid damaging the structure, and as a result, negligible energy in

16

the spectrum at frequencies higher than 25 kHz was found. Moreover, the dispersion

diagrams were not successful because of the unknown mechanical properties and layout

of the composite blade. Hence, it was difficult to discriminate vibration modes with

fundamental GW modes in this particular spectrum range. Moreover, as reported by

Moulin et al. [25], the duration time window T of the signals acquired must be higher

than the Heisenberg time τ_w or break time, which is equal to the modal density of the

structure. However, since is impossible to estimate τ_w due to the lack of knowledge of the

mechanical properties of the blade, according to the Nyquist theorem and the long

reverberation present in the waveforms recorded, a 100 ms duration time window T was

chosen (Fig. 2a). Sensor positions are reported in Table 1.

Table 1 Sensors coordinates

	x-coordinate (cm)	y-coordinate (cm)
Sensor 1	36	4
Sensor 2	40	4
Sensor 3	54	10
Sensor 4	58	10

V. IMPACT LOCALIZATION RESULTS

According to Section II, the structural surface was divided in M=17 x 6 excitation points,

distributed along a grid of rectangular cells (Fig. 1). The size of the single cell is not

constant, but varies from smaller cells of dimensions 6 cm x 2 cm on the GFRP region, to

greater cells of dimensions 6 cm x 3 cm on the CFRP section. Such a configuration was

designed to improve the resolution at the leading edge of the blade, as that is the area

mostly subjected to impacts. The refocusing wave fields at the impact source location are

represented as a 2D map and the maxima of Eq. (15) are deduced from highest values of the correlation coefficients (Fig. 5).
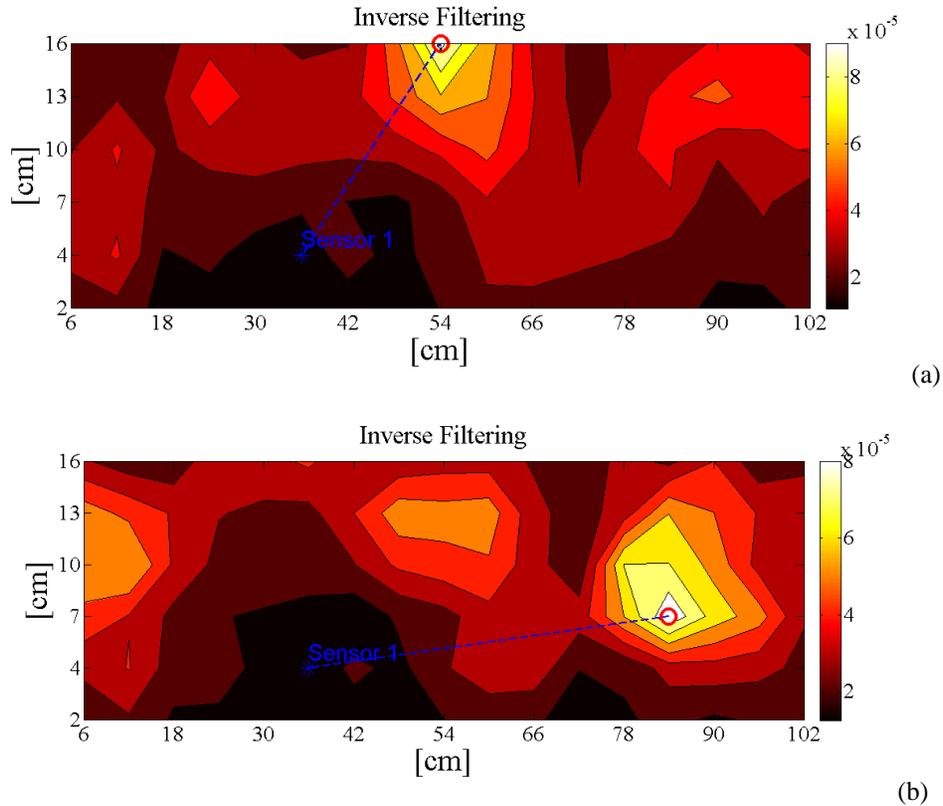

(a)

(b)

Figure 5 2D imaging of the impact location using only sensor 1 for two different impacts located at $x_1=54$ cm, $y_1=16$ cm (a) and $x_2=84$ cm, $y_1=7$ cm (b)

In the above figure, the asterisk symbol corresponds to the position of sensor 1, the red circle to the real impact location and the dashed blue line to the distance between the sensor and the impact point. However, it was found that for some excitation points, the incoherent measurement noise (e.g. sensor noise, electronic noise, etc…) could negatively influence the library of signals acquired in the first step, leading to ambiguities in the focusing at the source. This further effect was eliminated by acquiring simultaneously the wave fields in both steps with additional transducers, and then averaging the maxima of the correlation coefficients according to the following formula:

$$\hat{e}_{IF}\left(\mathbf{r}_m,\omega\right)=\frac{1}{N}\sum_{n=1}^{N}\left[\max\hat{e}_n\left(\mathbf{r}_m,\omega\right)\right] \qquad (17)$$

where N is the number of total sensors used in the IF process. In our tests, four sensors were used as they provided satisfactory results for the impact location in each excitation point (Figs. 6 and 7).
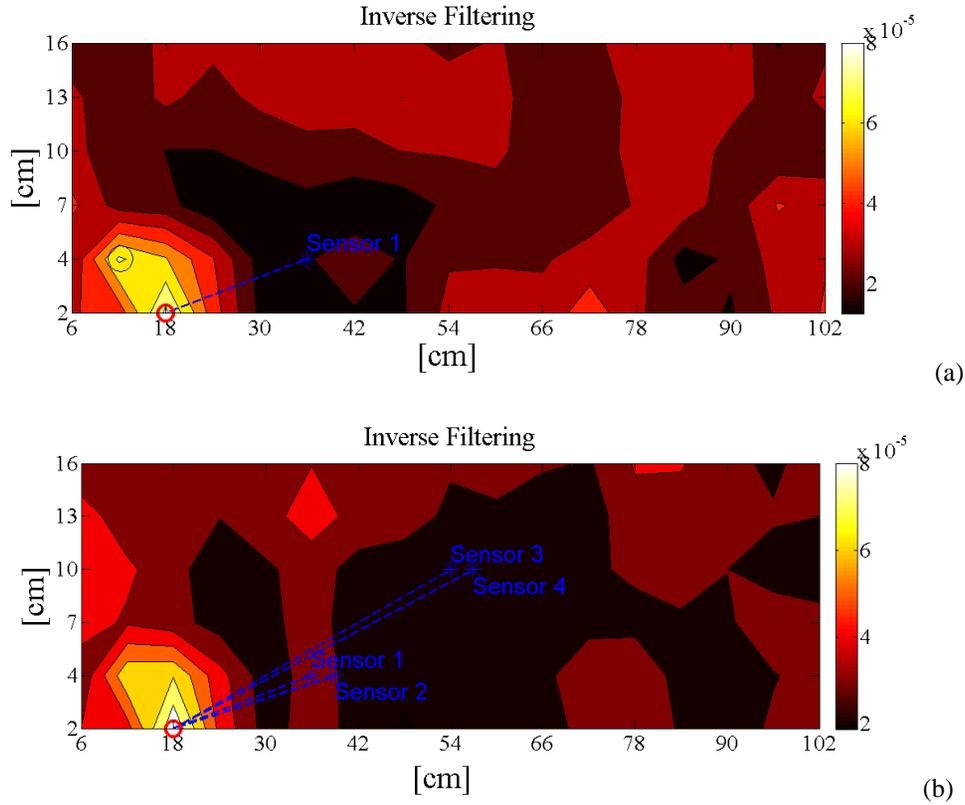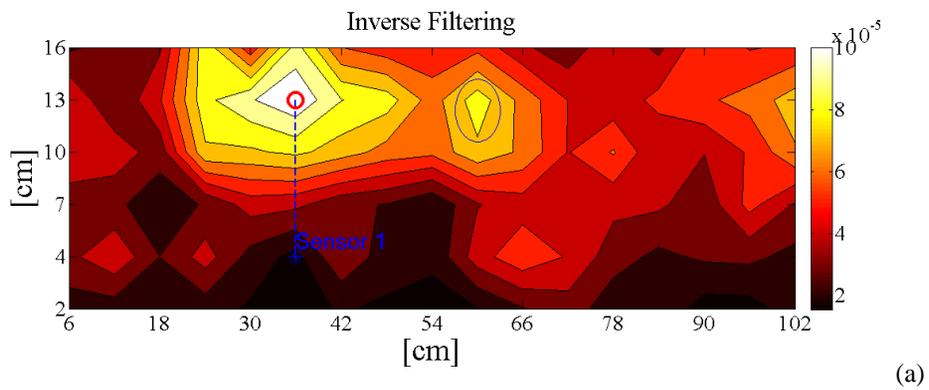

(a)

(b)

Figure 6 2D imaging of the impact location using only sensor 1 (a) and four sensors (b) for the impact located at x_1=18 cm, y_1=2 cm
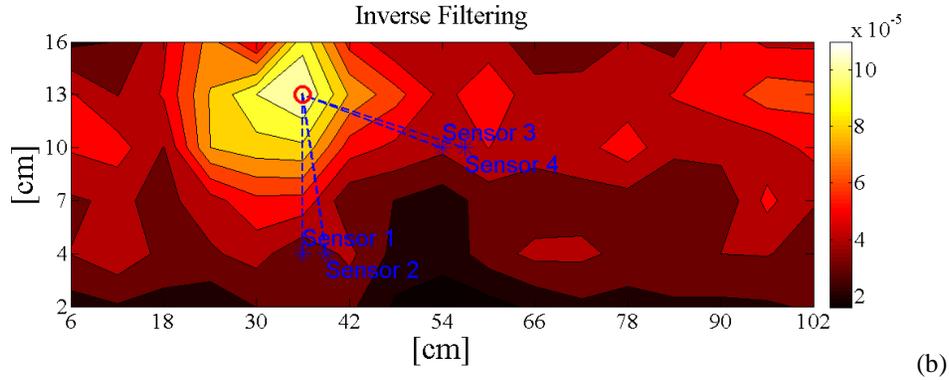

(a)

Figure 7 2D imaging of the impact location using only sensor 1 (a) and four sensors (b) for the impact located at $x_1=36$ cm, $y_1=13$ cm

Indeed, it can be seen from Figs. 6 and 7 that small ambiguities (highlighted by a blue circle) in the imaging of the impact source using only one sensor, were clearly resolved using the averaged values of the correlation coefficients from four receivers.

Hence compared to other ultrasonic impact localization techniques based on TOA evaluation, this methodology not only needs a simple signal processing to locate the source (with computational time less than 1 sec), but also it does not require any numerical routines as well as a priori knowledge of the mechanical properties and the GW dispersion behaviour. Further work is ongoing to test this imaging technique from the laboratory to a full-scale, operational activity.

VI. CONCLUSIONS

This paper proposes an in-situ Structural Health Monitoring (SHM) system for the localization of the impact source in real aerospace structures with diffuse field conditions. This technique, based on reciprocal time reversal process, is applied to a number of waveforms recorded by a number of passive sensors containing the impulse response of the medium. Unlike conventional ultrasonic impact localization systems based on the

20

time of arrival estimation, with the present method the benefits of scattering, mode conversions and boundary reflections enable the focusing at the impact source. Since the imaging process is obtained through a virtual focusing procedure, this system does not require any iterative algorithms and a priori knowledge of the mechanical properties of the structure and the anisotropic behaviour. The robustness of this technique was experimentally demonstrated on a tail rotor blade undergone to low velocity impacts. The imaging results showed that the location of the impact point could be achieved with a high level of accuracy in any point of the structure.

VII.   AKNOWLEDGEMENT

References:

[1] Ciampa F, Meo M. "Acoustic emission source localization and velocity determination of the fundamental mode A_0 using wavelet analysis and Newton-based optimization technique". *Smart Mater. Struct.* **19**, 1-14 (2010)

[2] De Marchi L, Marzani A, Speciale N, Viola E. "A passive monitoring technique based on dispersion compensation to locate impacts in plate-like structures". Smart Materials and Structures, **20** 035021 (2011)

[3] Ciampa F, Meo M. "A new algorithm for acoustic emission localization and flexural group velocity determination in anisotropic structures". Compos. Part A, **41**:1777–1786 (2010)

[4] Meo M, Zumpano G, Pigott M, Marengo G. "Impact identification on a sandwich plate from wave propagation responses". *Compos. Struct.* **71**, 302-306 (2005)

[5] Seydel R, Chang F.-K. "Impact identification on stiffened composite panels: system development". Smart Materials and Structures **10**, 354-369 (2001)

[6] Kosel T, Grabec I, Kosel F. "Intelligent location of simultaneously active acoustic emission sources". Aircraft Engineering and Aerospace Technology, **75**, No. 1, 11-17 (2003)

[7] Mustapha S., Ye L, Wang D, Lu Y. "Assessment of debonding in sandwich CF/EP composite beams using A0 Lamb wave at low frequency". Composite Structures **93**, 483 – 491 (2011)

[8] Gaul L, Hurlebaus S, Jacobs L -J. "Localization of a "synthetic" acoustic emission source on the surface of a fatigue specimen". Res. Nondestruct. Eval. **13**, 105-117 (2001)

[9] Ing R.-K, Quieffin N, Catheline S, Fink M. "In solid localization of finger impacts using acoustic time-reversal process". *Appl. Phys. Lett. 87*, 204104 (2005)

[10] Ciampa F, Meo M. "Impact detection in anisotropic materials using a time reversal approach". Structural Health Monitoring **11** (1), 43-49 (2012)

[11] Park H.-W, Kim S.-B, Sohn H. "Understanding a time reversal process in Lamb wave propagation" *Wave Motion, 56, 451–467*, (2009).

[12] Tanter M, Thomas J.-L, Fink M. "Focusing and steering through absorbing and aberrating layers: Application to ultrasonic propagation through the skull". *J. Acoust. Soc. Am. 103 (5)*, 2403–10 (1998).

[13] Ciampa F, Meo M. "Acoustic emission localization in complex dissipative anisotropic structures using a one-channel reciprocal time reversal method". J. Acoust. Soc. Am. **130** (1), 168-175 (2011)

[14] Landau L.D., Lifshitz E.M. Theory of elasticity, (2nd English ed.)Pergamon, New York (1960)

[15] Achenbach, J.D. Wave Propagation in Elastic Solids, NorthHolland, New York (1984)

[16] Duffy, D.G. Green's Function with Applications, CRC Press, Boca Raton (2001)

[17] Barton, G. Elements of Green Functions and Propagation: Potentials, Diffusion and Waves, Oxford Univ. Press, New York (1989)

[18] Cassereau D and Fink M. "Time-reversal of ultrasonic fields. III. Theory of the closed time-reversal cavity". *IEEE Trans. Ultrason. Ferroelectr. Freq. 39, 579–592* (1992).

[19] Catheline S, Queffin N, Ing R K, Fink M. "Acoustic source localization model using in-skull reverberation and time reversal". *Appl. Phys. Let. 90, 063902* (2007).

[20]   Weaver R. "On diffuse waves in solid media". *J. Acoust. Soc. Am. 71 (6)*, 1608–09 (1982).

[21]   Larose E, and Margerin L, Derode A, van Tiggelen B, Campillo M, Shapiro N, Paul A, Stehly L, Tanter M. "Correlation of random wavefields: An interdisciplinary review". Geophysics **71**, SI11-SI21 (2006)

[22]   Wapenaar K, Fokkema J, Snieder R. "Retrieveing the Green's function in an open system by cross correlation: A comparison of approaches (L)". *J. Acoust. Soc. Am. 118 (5)*, 2783–2786 (2005)

[23]   Fink M. "Time-reversal waves and super resolution". *Journal of Physics: Conference Series*, vol. **124**, p. 012004 (2008)

[24]   Qiu L, Yuan S , Zhang X, Wang Y. "A time reversal focusing based impact imaging method and its evaluation on complex composite structures". Smart Materials and Structures **20**, 105014 (2011)

[25]   Moulin E, Leyla N. A, Assaad J, Grondel S. "Applicability of acoustic noise correlation for structural health monitoring in nondiffuse field conditions". Applied Physics Letters **95**, 094104 (2009)